Josephson Effect in Hybrid Oxide Heterostructures with an Antiferromagnetic Layer

P. Komissinskiy,[1,2,3] G. A. Ovsyannikov,[1,2] I. V. Borisenko,[1] Yu. V. Kislinskii,[1] K. Y. Constantinian,[1] A. V. Zaitsev,[1] and D. Winkler[2]

[1]*Institute of Radio Engineering and Electronics, Russian Academy of Sciences, 125009 Moscow, Russia*
[2]*Department of Microtechnology and Nanoscience, Chalmers University of Technology, 41296 Gothenburg, Sweden*
[3]*Department of Materials Science, Darmstadt University of Technology, 64287 Darmstadt, Germany*

(Received 24 November 2006; revised manuscript received 30 April 2007; published 6 July 2007)

Josephson coupling between an *s*- and *d*-wave superconductor through a 50 nm thick $Ca_{1-x}Sr_xCuO_2$ antiferromagnetic layer was observed for the hybrid $Nb/Au/Ca_{1-x}Sr_xCuO_2/YBa_2Cu_3O_{7-\delta}$ heterostructures and investigated as a function of temperature, magnetic field, and applied millimeter-wave electromagnetic radiation. The magnetic field dependence of the *supercurrent* $I_c(H)$ exhibits anomalously rapid oscillations, which is the first experimental evidence of the theoretically predicted giant magneto-oscillations in Josephson junctions with antiferromagnetic interlayers.

DOI: 10.1103/PhysRevLett.99.017004 PACS numbers: 74.50.+r, 74.78.Fk, 75.70.Cn

The coexistence of superconducting and magnetic ordering in solids is of great interest for fundamental studies and electronic applications. In bulk compounds the exchange mechanism of ferromagnetic (FM) order tends to align spins of superconducting (S) Cooper pairs in the same direction preventing singlet superconducting pairing [1,2]. At the interfaces between superconducting and magnetic materials, however, superconducting and magnetic order parameters may interact due to the proximity effect resulting in interplay between superconducting and magnetic ordering and novel physical phenomena. For instance, superconductivity in ferromagnetic/superconducting/ferromagnetic (FM/S/FM) spin-valve junctions can be controlled by spin orientations in the FM electrodes [3]. Another effect is the damped oscillatory behavior of the superconducting order parameter induced in the ferromagnetic layer across S/FM interfaces that may lead to a π phase shift in the *supercurrent* of S/FM/S Josephson junctions [4].

We would expect interesting mesoscopic physical effects also at interfaces between superconductors and antiferromagnets (AFM). Monotonous suppression of the superconducting order parameter at the S/AFM interface with band-type AFM and novel low-energy Andreev bound states originating from spin dependent quasiparticle reflections at S/AFM interfaces have been theoretically predicted [5,6]. The observation of the Josephson effect in Nb/Cu/FeMn/Nb polycrystalline thin film heterostructures has been demonstrated in [7], where the γ-$Fe_{50}Mn_{50}$ alloy was used as metallic AFM layer. Although strong suppression of superconductivity has been observed in AFM FeMn layers similar to the ferromagnetic case, the supercurrent modulation with an applied magnetic field $I_c(H)$ shows rather conventional Fraunhofer pattern [7]. If, instead, the polycrystalline metallic AFM is substituted by an array of ferromagnetic layers with alternating directions of magnetization, then according to the theoretical calculations by Gor'kov and Kresin the $I_c(H)$ dependence should exhibit rapid oscillations originating from a gradual weak canting of the magnetic moments in the presence of an applied magnetic field [8].

Investigations of S/AFM interfaces composed of oxide high-temperature superconductors (HTS) and antiferromagnetic materials are relevant in order to understand the pairing mechanism of high-temperature superconductivity. No superconducting pairing has been found experimentally in $La_{1.85}Sr_{0.15}CuO_4/La_2CuO_4/La_{1.85}Sr_{0.15}CuO_4$ S/AFM/S heterostructures with a one-unit-cell thick antiferromagnetic insulator La_2CuO_4, thus, counteracting the mixing of antiferromagnetism and high-temperature superconductivity [9]. If the La_2CuO_4 barrier is doped across the insulator-metal transition and becomes HTS itself ($La_2CuO_{4+\delta}$), the "giant proximity effect," namely, a pronounced Josephson supercurrent, has been observed in the S/N′/S heterostructures above the superconducting transition temperature of the $La_2CuO_{4+\delta}$ N′ barrier with a thickness of up to 20 nm, which is well beyond the short coherence length of the cuprates [10]. In [10] the "giant proximity effect" is explained by resonant tunneling through the pair states in the barrier. The alternative explanation has been suggested in [11], where the experimentally obtained high value of the supercurrent is explained by the presence of microshorts through the interlayer.

In spite of recently renewed interest in superconducting structures with magnetically active materials, there is still a lack of experimental results on Josephson junctions with antiferromagnetic weak links, in particular, comprised of oxide HTS and AFM materials. For instance, no experimental observations of the theoretically predicted rapid oscillations of $I_c(H)$ have been demonstrated so far [8].

Here we report on the experimental studies of dc and rf current transport in hybrid thin film S-N-AFM-D antiferromagnetic junctions fabricated in the form of $Nb/Au/Ca_{1-x}Sr_xCuO_2/YBa_2Cu_3O_{7-\delta}$ mesa heterostructures with areas from 10×10 up to 50×50 μm^2 [see inset (a) of Fig. 1] [12,13]. Here Nb is a conventional *s*-wave superconductor (S), $YBa_2Cu_3O_{7-\delta}$ (YBCO) is an oxide *d*-wave superconductor (D), Au is a normal metal

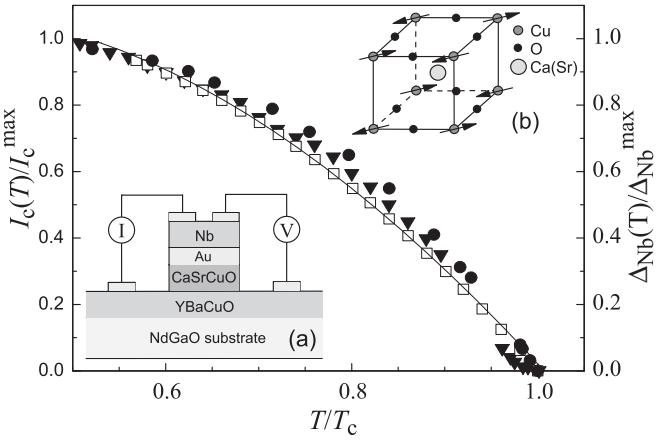

FIG. 1. Temperature dependences of the supercurrents $I_c(T)$ of the AFM junction no. 1 (circles), no. 2 (triangles), and the Nb/Au/YBCO junction no. 6 (squares). The $I_c(T)$ dependences are normalized by $I_c^{max} \equiv I_c(4.2\ \mathrm{K})$. The approximation of temperature dependence of Nb superconducting gap $\Delta_{Nb}(T)$ experimentally determined from the I-V curves of the Nb/Au/YBCO junction is shown by the solid line. T and $\Delta_{Nb}(T)$ are normalized by critical temperature of the Josephson junctions and $\Delta_{Nb}^{max} \equiv \Delta_{Nb}^{max}(4.2\ \mathrm{K}) = 1.1$ meV, respectively. Inset (a) is a sketch of the AFM-junction geometry and used measurement scheme. Inset (b) is a sketch of the CSCO AFM structure.

(N), and $Ca_{1-x}Sr_xCuO_2$ (CSCO) is a quasi-two-dimensional Heisenberg AFM, where the quasiparticle spin direction alternates in the neighbor {111} ferromagnetic planes [see inset (b) of Fig. 1] [14]. Taking into account weak magnetic coupling between the neighbor magnetic planes we can consider current transport along ⟨111⟩ CSCO being equivalent to the case of an A-type AFM layer suggested in [8]. Electric and electronic paramagnetic resonance measurements of the CSCO thin films in the temperature range of 4.2–300 K demonstrate hopping conductivity and a Néel temperature $T_{Neel} =$ 90–120 K, respectively [15]. Thus, the CSCO films are in a G-type antiferromagnetic Mott-insulating state within the temperature range of 4.2–40 K, where the electrical measurements presented in this Letter have been carried out.

In order to avoid microshorts in the AFM junctions, several precautions were taken: (i) the deposited CSCO films ($d_{cs} = 20$ or 50 nm) are thicker than the rms surface roughness of the YBCO layer; (ii) the Nb/Au bilayer is used as superconducting counterelectrode in our junctions. Direct Nb deposition on top of the CSCO/YBCO heterostructure results in the formation of a Nb/CSCO interface with very high resistance ($\sim 1\ \Omega\ \mathrm{cm}^2$) due to Nb oxidation. Thus, if the Au layer was locally damaged because of the finite surface roughness of the CSCO/YBCO heterostructure, then a high resistivity niobium oxide is formed to heal any shunting conductivity at that point.

A 4-point measurement technique was used for electrical characterization of our AFM junctions with two contacts to the YBCO electrode and two contacts to the Nb counterelectrode [see inset (a) of Fig. 1]. The difference in electronic parameters of Au and CSCO and the surface characteristics of the CSCO/YBCO bilayer determine the potential barrier I_b at the Au/CSCO interface and the junction resistance [16]. Thus, our AFM junction can be considered as an S/N/I_b/AFM/D structure, where the superconducting order parameter is induced in the normal Au and the AFM CSCO layers by the proximity effect to Nb and YBCO electrodes, respectively [17].

Figure 1 shows temperature dependences of the supercurrent $I_c(T)$ obtained using dc transport measurements of the AFM junction. The $I_c(T)$ dependence of a Nb/Au/YBCO junction ($d_{cs} = 0$) is presented for comparison. We observe a good qualitative agreement of all normalized $I_c(T)$ dependences with the temperature dependence of the Nb superconducting gap (Δ_{Nb}) derived from the I-V curve of the Nb/Au/YBCO junction (solid line in Fig. 1) [17]. However, the $I_c(T)$ curve does not follow a dependence typical for S/N/S junction and the values of $V_c \equiv I_c R_N$ (R_N is resistance of the junction in the normal state) calculated from the I-V curves of different samples do not show any pronounced dependence on d_{cs} [18]. Thus, we may conclude that the superconducting coherence length in the CSCO AFM layer ξ_{AFM}, which determines the penetration depth of the superconducting ordering in the AFM layer, is not small with respect to the thickness of the CSCO layer d_{cs}. A qualitative estimation of ξ_{AFM} in the case of ballistic electron transport (quasiparticle mean free path $l > d_{cs}$) can be performed by modeling of the AFM as a stack of -FM-FM′-FM-FM′- thin ferromagnetic layers FM and FM′ with alternating direction of exchange field $\xi_{AFM} \sim \min\{l, h\nu_F/(2\pi kT)\}$ [8], where ν_F is the quasiparticle Fermi velocity, h and k are the Planck and Boltzmann constants, respectively. Thus, we obtain $\xi_{AFM} \approx 7$ nm at $T = 4.2$ K for one of the measured AFM junctions. Note that the value of ξ_{AFM} depends on the properties of the CSCO AFM layer (oxygen content, Fermi velocity, mean free path, etc.) and might vary in different experimental samples.

Our experimental data show that I_c and R_N of the AFM junctions vary considerably between the samples since the transparency value of the Au/CSCO interface is not technologically reproducible (see Table I). However I_c and R_N are the correlated parameters and the values of V_c in the different AFM junctions are consistent and systematically 2–3 times higher than those of the Nb/Au/YBCO junctions. Thus, one can conclude that the reason for the observed enhancement of the supercurrent in the AFM junctions is related to the presence of the AFM CSCO interlayer. A possible reason for this enhancement is the complex superconducting order parameter in YBCO thin films with the dominant d-wave and minor s-wave components [19]. The latter arises even in the bulk, in particular, because of orthorhombic crystal structure of YBCO [17,19]. However, change of symmetry of the superconducting order parameter may occur across the AFM/D interface in the AFM junctions. For instance, the d-wave

TABLE I. Parameters of the AFM junctions at $T = 4.2$ K and $H = 0$. d_{cs} is the thickness of the $Ca_{1-x}Sr_xCuO_2$ interlayer, x characterizes the Sr doping level in $Ca_{1-x}Sr_xCuO_2$. Parameters A, I_c, R_N, and $V_c = I_cR_N$ are the area, supercurrent, normal resistance, and characteristic voltage of the junctions, respectively.

Sample no.	d_{cs} (nm)	x	A (μm^2)	I_c (μA)	R_N (Ω)	V_c (μV)
1	20	0.5	10×10	400	0.8	320
2	50	0.15	20×20	555	0.4	222
3	50	0.15	10×10	48	3.5	170
4	50	0.5	50×50	70	2.9	203
5	0	0	50×50	270	0.2	54
6	0	0	20×20	18	3.6	65

symmetrical component of the superconducting pairing of YBCO may be transformed across the CSCO/YBCO interface into a superposition of the spin-triplet p_x-wave and the extended s-wave components, thus, enhancing the values of V_c [20].

In S/FM/S Josephson junctions the ''giant Josephson effect'' caused by an anomalously large penetration of the superconducting order parameter into the ferromagnetic layer with spiral-type magnetization may be explained by a triplet superconducting pairing generated at the S/FM interface between the s-wave superconductor and the ferromagnetic film [2,21]. We emphasize that in our case, unlike [21], the value of the Josephson supercurrent may be qualitatively explained only by a singlet s-wave component of the superconducting pairing induced at the CSCO/YBCO interface. Moreover, low-energy Andreev bound states at the CSCO/YBCO interface may act as an additional channel for the supercurrent in our AFM junctions [6].

Integer and half-integer Shapiro steps at voltages $V_n = n(hf_e/2e)$ and $V_{n-1/2} = (n - 1/2)hf_e/2e$ ($n = 1, 2, 3, \ldots$), respectively, are observed in the I-V curves of the investigated AFM junctions irradiated by an external millimeter-wave electromagnetic source at frequencies $f_e = 36$–120 GHz (see Fig. 2 for $f_e = 56$ GHz). The oscillating dependences of the critical current, $I_c(I_e)$, and the amplitudes of the Shapiro steps, $I_n(I_e)$, versus the millimeter-wave electromagnetic current amplitude I_e were derived from the I-V curves of the AFM junctions (Fig. 3). Values of I_e were calculated as the square root of power of the external radiation. The experimentally obtained $I_c(I_e)$ dependences follow the resistively shunted junction (RSJ) model of Josephson junctions, where electrical current of the junction is considered as superposition of superconducting and quasiparticle parts [22].

In the high frequency limit of the RSJ model $f_e > f_c = (2e/h)I_cR_N$ the $I_c(I_e)$ dependence is proportional to zero order of the modified Bessel function $\mathcal{J}_0(2\alpha)$ and, similarly, $I_n(I_e) \propto \mathcal{J}_n(2\alpha)$, where $\alpha = eI_eR_N/hf_e$. Good approximation of the experimentally obtained $I_1(I_e)$ dependence by our simulations within the RSJ model is a supplementary indication of the absence of microshorts in the AFM junctions and Josephson origin of the supercurrent. The absence of excess currents in the I-V curves of the AFM junctions is further evidence against the formation of microshorts [17]. The half-integer Shapiro steps (Fig. 2) may originate from a second harmonic component ($I_{c2}\sin 2\varphi$) in superconducting current-phase relation of the AFM junctions [$I(\varphi) = I_{c1}\sin\varphi + I_{c2}\sin 2\varphi$] as well as from their finite capacitance C [Stewart-McCumber parameter $\beta_c = (2e/h)\, I_cR_N{}^2C$] [23]. The modified RSJ model, which takes into account nonzero values of C and I_{c2} fit well the experimental $I_c(I_e)$ and $I_1(I_e)$ curves in Fig. 3 [24]. In particular, the I_{c2} value used to fit the experimentally obtained $I_c(I_e)$, $I_1(I_e)$, and $I_{1/2}(I_e)$ curves (Figs. 2 and 3) is as high as $q = I_{c2}/I_{c1} = 0.2$ [24].

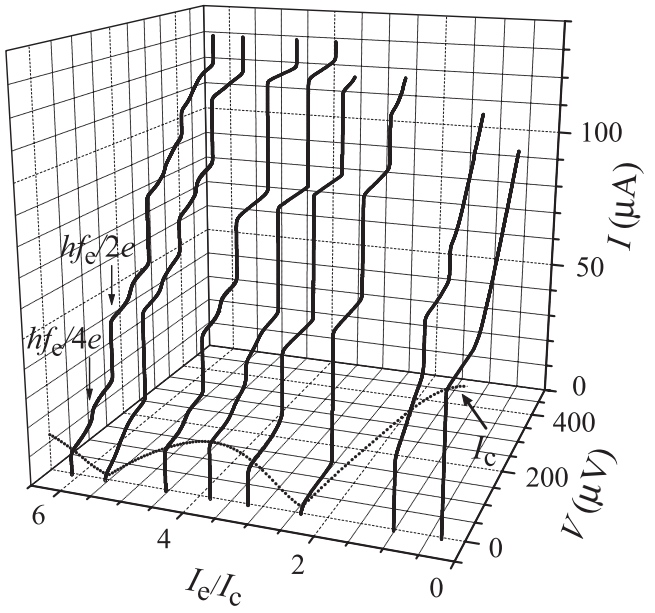

FIG. 2. I-V curves of the AFM junction no. 3 at the applied millimeter-wave electromagnetic current (I_e) at $f_e = 56$ GHz and $T = 4.2$ K (solid lines). Positions of one integer and one half-integer Shapiro steps are denoted. $I_c(I_e)$ dependence calculated within the RSJ Josephson junction model is shown for comparison (dotted line).

Figure 4 shows $I_c(H)$ dependences of an AFM junction and a Nb/Au/YBCO junction of the same area 50×50 μm^2. The I_c values in Fig. 4 were obtained from the dc measurements of the I-V curves. In order to perform high sensitivity magnetic field measurements in the microTesla range we used a magnetic field coil with a dc source and amorphous multiturn μ-metal shielding. The magnetic field is applied parallel to the thin film surfaces, i.e., in plane of the Josephson junction. The widths H_0 of the central I_c peaks of the $I_c(H)$ curves are 3.2 and 88 μT for the AFM junction and the Nb/Au/YBCO junction, respectively. Another specific feature of the AFM junction is the additional rapid modulation of the $I_c(H)$ pattern with a period of $H_1 \approx 0.7$ μT, which is about 5 times smaller

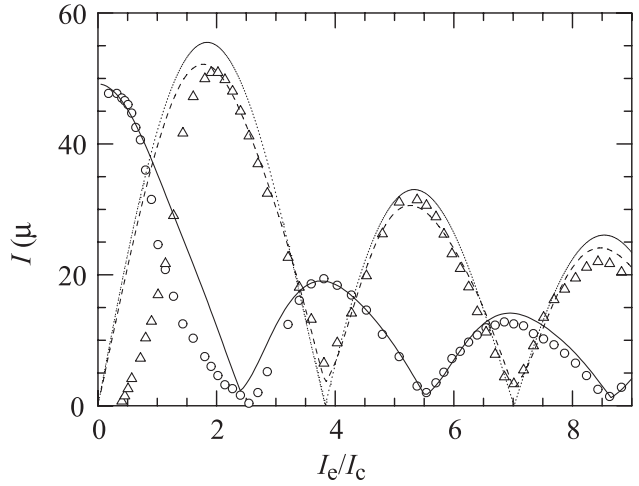

FIG. 3. Dependences of the supercurrent [$I_c(I_e)$, circles] and the first integer Shapiro step [$I_1(I_e)$, triangles] versus the applied millimeter-wave electromagnetic current I_e. The data are derived from the I-V curves of the AFM junction no. 3 at $f_e = 56$ GHz and $T = 4.2$ K. The solid and dashed lines correspond to the $I_c(I_e)$ and $I_1(I_e)$ curves numerically calculated from the modified RSJ model with $q = I_{c2}/I_{c1} = 0.2$ [24]. The dotted line shows the calculated $I_1(I_e)$ dependence for $q = 0$, i.e., $I_1 \propto \mathcal{J}_1(2\alpha)$, where $\mathcal{J}_1$ is a first order Bessel function and $\alpha = eI_eR_N/hf_e$.

than the H_0. The shape of the rapid oscillations strongly depends on the direction of the applied magnetic field. For instance, in-plane rotation of the applied magnetic field H by 90° makes the $I_c(H)$ pattern asymmetric and doubles H_0 and H_1. Thus, the observed rapid oscillations of $I_c(H)$ qualitatively correspond to the theoretically predicted ones

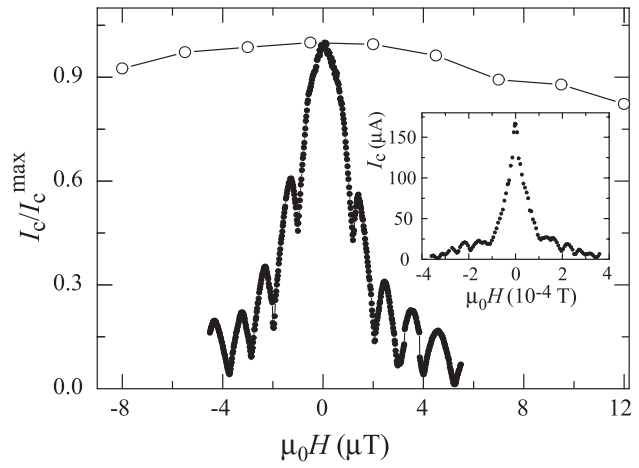

FIG. 4. Magnetic field dependences of the supercurrent $I_c(H)$ of the AFM junction no. 4 (filled circles) and the Nb/Au/YBCO junction no. 5 (open circles) at 4.2 K. The I_c is normalized by $I_c^{max} \equiv I_c(4.2\ \mathrm{K})$. The inset shows a large-scale $I_c(H)$ graph of the Nb/Au/YBCO junction [25].

in the case of S/AFM/S Josephson junctions with layered AFM with alternating magnetic moments [8].

In conclusion, we have experimentally demonstrated dc and ac Josephson effects in Nb/Au/CSCO/YBCO thin film junctions with antiferromagnetic CSCO layers. Values of the Josephson characteristic voltage $V_c = I_cR_N \sim 100$–$200\ \mu$V were demonstrated in the Nb/Au/CSCO/YBCO junctions with up to 50 nm thick CSCO AFM layer. The ac Josephson effect is manifested in multiple Shapiro steps, which are well fitted by the RSJ Josephson junction model. The experimentally observed rapid oscillations of $I_c(H)$ dependence qualitatively agree with the theory [8].

The authors are grateful to V. V. Demidov, F. Lombardi, V. A. Luzanov, I. M. Kotelyanski, and U. Poppe for helpful discussions. This work was supported by the Russian Academy of Sciences, the ESF AQDJJ and THIOX, Swedish KVA, SI and SSF "OXIDE," and EU NANOXIDETTC.

[1] A. I. Buzdin, Rev. Mod. Phys. **77**, 935 (2005).
[2] F. S. Bergeret *et al.*, Rev. Mod. Phys. **77**, 1321 (2005).
[3] J. Y. Gu *et al.*, Phys. Rev. Lett. **89**, 267001 (2002).
[4] V. V. Ryazanov *et al.*, Phys. Rev. Lett. **86**, 2427 (2001).
[5] V. N. Krivoruchko, Zh. Eksp. Teor. Fiz. **109**, 649 (1996) [Sov. Phys. JETP **82**, 347 (1996)].
[6] B. M. Andersen *et al.*, Phys. Rev. B **72**, 184510 (2005).
[7] C. Bell *et al.*, Phys. Rev. B **68**, 144517 (2003).
[8] L. Gor'kov and V. Kresin, Appl. Phys. Lett. **78**, 3657 (2001).
[9] I. Bozovic *et al.*, Nature (London) **422**, 873 (2003).
[10] I. Bozovic *et al.*, Phys. Rev. Lett. **93**, 157002 (2004).
[11] K.-U. Barholtz *et al.*, Physica (Amsterdam) **334C**, 175 (2000).
[12] G. A. Ovsyannikov *et al.*, JETP Lett. **84**, 262 (2006).
[13] We have observed no deviation of dc and rf properties of the AFM junctions deposited on differently oriented $NdGaO_3$ substrates. Thus, we do not include the thin film orientation issue in the following discussion of the obtained experimental data.
[14] M. Matsumura *et al.*, Phys. Rev. B **60**, 6285 (1999).
[15] G. A. Ovsyannikov *et al.*, Physica (Amsterdam) C (to be published).
[16] F. V. Komissinskii *et al.*, Phys. Solid State **43**, 801 (2001).
[17] P. V. Komissinski *et al.*, Europhys. Lett. **57**, 585 (2002).
[18] K. A. Delin and A. W. Kleinsasser, Supercond. Sci. Technol. **9**, 227 (1996).
[19] C. C. Tsuei and J. R. Kirtley, Rev. Mod. Phys. **72**, 969 (2000).
[20] K. Kuboki, Physica (Amsterdam) **284–288B**, 505 (2000).
[21] R. S. Keizer *et al.*, Nature (London) **439**, 825 (2006).
[22] K. K. Likharev, Rev. Mod. Phys. **51**, 101 (1979).
[23] A. A. Golubov *et al.*, Rev. Mod. Phys. **76**, 411 (2004).
[24] Yu. V. Kisliskii *et al.*, JETP **101**, 494 (2005).
[25] The smaller $I_c = 165\ \mu$A for the junction 5 presented in Fig. 4 was measured after multiple cooling cycles 2 years later than $I_c = 270\ \mu$A given in Table I.